A miR-340/SPP1 axis inhibits the activation and proliferation of hepatic stellate cells by inhibiting the TGF-β1/Smads pathway

Ronghua Zhang[1,A,D], Meimei Wang[1,B,C], Hongjian Lu[1,B], Jingyao Wang[2,B], Xiangyang Han[1,B], Zhiyong Liu[3,C], Lin Li[1,C], Mingming Li[1,B,D], Xiaoli Tian[4,B], Shuang Chen[5,C], Guangling Zhang[2,A,E,F], Yanan Xiong[1,A,E], Jingwu Li[6,D,F]

[1] Hebei Key Laboratory for Chronic Diseases, School of Basic Medical Sciences, North China University of Science and Technology, Tangshan, China
[2] School of Clinical Medicine, North China University of Science and Technology, Tangshan, China
[3] Health Science Center, North China University of Science and Technology, Tangshan, China
[4] Gastroenterology Department, Tangshan Paraplegia Sanatorium, China
[5] Tianjin Key Laboratory of Early Druggability Evaluation of Innovative Drugs, Tianjin International Joint Academy of Biomedicine, China
[6] The Cancer Institute, Hebei Key Laboratory of Molecular Oncology, Tangshan People's Hospital, China

A – research concept and design; B – collection and/or assembly of data; C – data analysis and interpretation;
D – writing the article; E – critical revision of the article; F – final approval of the article

Advances in Clinical and Experimental Medicine, ISSN 1899–5276 (print), ISSN 2451–2680 (online) *Adv Clin Exp Med*. 2023;32(4):469–479

Address for correspondence
Guangling Zhang
E-mail: zhanggl@ncst.edu.cn

Conflict of interest
None declared

Acknowledgements
The authors would like to thank Professors Yankun Liu and Yufeng Li (Tangshan People's Hospital, China) for providing human primary normal fibroblasts. The authors thank AiMi Academic Services (www.aimieditor.com) for the English language editing and review services.

Received on December 13, 2021
Reviewed on August 8, 2022
Accepted on September 28, 2022

Published online on November 22, 2022

Cite as
Zhang R, Wang M, Lu H, et al. A miR-340/SPP1 axis inhibits the activation and proliferation of hepatic stellate cells by inhibiting the TGF-β1/Smads pathway. *Adv Clin Exp Med*. 2023;32(4):469–479. doi:10.17219/acem/154996

DOI
10.17219/acem/154996

Abstract

Background. Hepatic fibrosis (HF) is a common pathological complication of liver cirrhosis which affects human health. It is well established that microRNAs (miRNAs) regulate the proliferation, activation and apoptosis of hepatic stellate cells (HSCs).

Objectives. To determine the function and molecular mechanism of miR-340-5p/secreted phosphoprotein 1 (SPP1) axis in HF and identify potential therapeutic targets.

Materials and methods. The HF model in cholestatic rats was induced by ligating the common bile duct. The histological sections of the liver tissues were stained with hematoxylin and eosin (H&E), Masson's trichrome or Sirius Red. The differential expression of mRNAs in the liver tissues was examined using the microarray analysis. The expression levels of miR-340-5p, SPP1, alpha-smooth muscle actin (α-SMA), Collagen I, phosphorylated Smad2 (p-Smad2), and p-Smad3 were determined using quantitative real-time polymerase chain reaction (qRT-PCR) or western blot. Cell proliferation was quantified using cell counting kit-8 (CCK-8) assays. The regulatory effect of miR-340-5p on SPP1 was determined with fluorescent reporter assay.

Results. The bile duct ligation (BDL) rat model was successfully induced, and SPP1 was upregulated in liver tissue from the BDL group compared to that of the sham group. The expression level of miR-340-5p was decreased in activated human primary normal fibroblasts (NFs) and activated LX-2 cells, and the mRNA and protein expression levels of SPP1 were increased in activated LX-2 cells. The SPP1 was the target of miR-340-5p, and the overexpression of SPP1 increased the proliferation of LX-2 cells, the expression of HF markers α-SMA and Collagen I, and key factors p-Smad2 and p-Smad3 (all $p < 0.05$). However, reverse results were obtained with the overexpression of miR-340-5p in LX-2 cells.

Conclusions. Our findings provide evidence that SPP1 targeted by miR-340-5p promotes LX-2 cell proliferation and activation through the TGF-β1/Smads signaling pathway. Therefore, miR-340-5p and SPP1 may be possible therapeutic targets for HF.

Key words: hepatic fibrosis, hepatic stellate cells, miR-340-5p, TGF-β1 signaling, secreted phosphoprotein 1

Funding sources
The study was funded by the Government Funded Clinical Medicine Talents Training Project of Hebei Province (grant No. [2020] 397), the Natural Science Foundation of Hebei Province (grant No. H2021209026), Returned Overseas Students of Hebei Province (grant No. C20210340), Key Research and Development, Innovation and Improvement Projects of Hebei Province (grants No. 213777115D and 205A7701H), Science and Technology Project of Hebei Education Department (grant No. JQN2020005), and the National Natural Science Foundation of China (grant No. 81972746).

Background

Hepatic fibrosis (HF) is a pathological complication of many liver diseases. It is generally associated with chronic hepatic inflammation and injury. In HF, hepatic stellate cells (HSCs) are activated to produce extracellular matrix (ECM), which becomes fibrous and accumulates.[1] Hepatic stellate cells are activated by several signalling pathways, including canonical tissue growth factor β1 (TGF-β1),[2] which is established in HF.[3] However, the complexity of HSC activation has limited the understanding of the regulatory mechanisms, which hinders the therapeutic options for HF.[4] Thus, clarifying this regulatory mechanism is essential for the development of effective antifibrotic therapy.

MicroRNAs (miRNAs) regulate the physiological and pathological process of fibrotic diseases by directly interfering with the expression of their functional target genes, especially genes affecting organs, such as liver, kidney, lung, or heart.[5] Hepatic stellate cells are activated and transformed by many miRNAs, highlighting miRNAs as potentially suitable targets for the treatment of HF. One example is miR-942, which mediates the activation of HSCs by downregulating bone morphogenic protein (BMP) and activin membrane-bound inhibitor (BAMBI) in human HF.[6] Also, miR-455-3p alleviates the activation of HSCs and HF by inhibiting the expression of heat shock transcription factor 1 (HSF1).[7] The miR-340-5p alleviates lung fibrosis by targeting the TGF-β/P38/ATF1 signaling pathway,[8] and the transplantation of bone marrow mesenchymal stem cell-derived exosomes containing miR-340-5p reduces endometrial fibrosis.[9] However, the effects of miR-340-5p in the process of HSC activation in human HF remain unknown.

In this study, a bile duct ligation (BDL) HF rat model was successfully induced and a microarray analysis was performed to identify genes involved in the pathophysiology of HF. One such gene highly upregulated in the liver of BDL rats was the secreted phosphoprotein 1 (*SPP1*) gene. Recent studies have revealed that *SPP1* is upregulated in various human fibrotic diseases,[10–12] and that several miRNAs, such as miR-539-5p,[13] miR-186[14] and miR-181c,[15] regulate *SPP1* expression. Therefore, we tested the possible involvement of the overexpression of *SPP1* in HF and its regulation by miR-340-5p.

Objectives

To determine the interactions between miR-340-5p and *SPP1* in HF and identify potential therapeutic targets.

Materials and methods

BDL rat model

The use of all animals was approved by the Laboratory Animal Ethics Committee of North China University of Science and Technology, Tangshan, China (approval No. LAEC-NCST-2020187). A total of 14 male Sprague Dawley rats (age: 8 weeks; weight: 210–260 g) (Beijing HFK Bioscience Co., Ltd., Beijing, China) were divided into the BDL group (n = 7) and sham group (n = 7), and maintained at 23 ±2°C with free access to water and food. Animals were anesthetized, and those in the BDL group underwent a common bile duct separation and ligation to establish the model, while the sham group rats underwent a laparotomy to separate the duct without ligation. Incisions were treated with penicillin, and rats were kept flat until the anesthesia subsided. On the 14th day after the operation, the rats were sacrificed by exsanguination through the abdominal aorta after anesthesia, the blood and liver tissues were collected by flash freezing in liquid nitrogen, and liver tissues were preserved in RNAlater™ Stable preservation solution of animal tissue RNA (Beyotime, Shanghai, China) at –80°C until used.

Serum enzymes

The Comprehensive Diagnostic Profile kit on a VetScan VS2 (Abaxis Inc. North America, Union City, USA) was used to determine the levels of liver injury markers, including serum alanine aminotransferase (ALT), aspartate aminotransferase (AST), total bile acid (TBA), and total bilirubin (TBIL).[16]

Liver histology

Livers were paraffin-embedded, cut into 5-µm-thick sections, deparaffinized and rehydrated, followed by staining with hematoxylin and eosin (H&E; Beijing Yili Fine Chemicals Co., Ltd., Beijing, China), Masson's trichrome (PhyEasy™ Masson Staining Kit, PH1427; Phygene, Fujian, China) or Sirius Red (Picro Sirius Red Stain Kit, ab150681; Abcam, Cambridge, UK), or subjected to immunohistochemistry (Gibco, Thermo Fisher Scientific, Waltham, USA), according to the manufacturer's instruction. For immunohistochemistry, the sections were covered with prepared ethylenediaminetetraacetic acid (EDTA) solution (Wanleibio, Shenyang, China), and repaired under high pressure for 3 min. This was followed by applying peroxidase blocking agent (ReportBio, Hebei, China) for 10 min, and washing with phosphate-buffered saline (PBS). Subsequently, they were incubated with alpha-smooth muscle actin (α-SMA) primary antibodies (ab5694, 1:200; Abcam), then with a biotin-labeled secondary antibody (ab6721, 1:500; Abcam), and finally stained with diaminobenzidine tetrahydrochloride.

mRNA microarray and the determination of differentially expressed genes

Differential mRNA expression in the liver tissue of BDL and sham groups (n = 3) was analyzed using a Rat Gene Expression Microarray (Agilent Technologies, Santa Clara,

USA) with an 8 × 60K chip. The TIFF format image data file of the Agilent mRNA expression chip following hybridization scanning was preprocessed and analyzed using feature extraction software (method No. AG-GE-WL02-01-2012, data analysis method No. AG-GEDL00-01-2010; CapitalBio Technology, Beijing, China).

Cell culture

The use of human primary normal fibroblasts (NFs) was authorized by the Ethics Committee of Tangshan People's Hospital, China (approval No. RMYY-LLKS-2020-002).[17] The cells were cultured in Dulbecco's modified Eagle's F12 medium (DMEM/F12; Thermo Fisher Scientific) containing 10% epidermal growth factor, 20% fetal bovine serum (FBS) and 1% penicillin/streptomycin (P/S) (Minhai Biotechnology Co., Ltd., Beijing, China). The immortalized human hepatic stellate LX-2 cell line was obtained from Peking Union Medical College (Beijing, China) and cultured in Dulbecco's modified Eagle's medium (DMEM; Tianjin Meiji Chemical Co., Ltd., Tianjin, China) containing 1% P/S and 10% FBS. All cells were cultured and kept in an incubator with 5% CO_2 at 37°C. To further activate cells, they were treated with 10 ng/mL TGF-β1 (PeproTech, Inc., Cranbury, USA) for 24 h, as previously described.[18]

miRNA target prediction

The miRNA potential target genes were predicted using TargetScan (targetscan.org/vert_72/) and miRDB (https://mirdb.org/mirdb/index.html).[19]

Quantitative real-time polymerase chain reaction

TRIzol reagent (Invitrogen, Thermo Fisher Scientific) was used to extract the total RNA from tissues and cells following the manufacturer's protocol. NanoDrop™ 2000 spectrophotometer (Thermo Fisher Scientific) was used to measure the total RNA concentration. Next, cDNAs were synthesized using an mRNA reverse transcription kit (Mei5 Biotechnology Co., Ltd., Beijing, China) or miRNA First Strand cDNA Synthesis kit (Sangon Biotech, Shanghai, China), with the latter kit using miRNA universal reverse primers. The Prime Script RT-PCR kit (TaKaRa, Kusatsu, Japan) and SYBR Select Master Mix (Thermo Fisher Scientific) were used for quantitative real-time polymerase chain reaction (qRT-PCR), and the reactions were performed on an ABI 7500 Fast Real-Time PCR system (Applied Biosystems, Thermo Fisher Scientific). The qRT-PCR reaction conditions were set at 95°C for 3 min, and then 40 cycles at 95°C for 15 s, 60°C for 35 s and 72°C for 30 s. The $2^{-\Delta\Delta Ct}$ method was used to analyze the relative expression of the genes, with experiments being performed in triplicate. The mRNA expressions of Collagen I, α-SMA and SPP1 were normalized to glyceraldehyde 3-phosphate dehydrogenase (GAPDH), and miR-340-5p was normalized to U6, expression of GAPDH and U6 were set to 1. The primer sequences were as follows:

GAPDH forward
(F): 5'-CCGCATCTTCTTGTGCAGTG-3',
and GAPDH reverse
(R): 5'-TCCCGTTGATGACCAGCTTC-3';
U6 F: 5'-CTCGCTTCGGCAGCACATA-3';
miR-340-5p F: 5'-GCGGTTATAAAGCAATGAGA-3';
SPP1 F: 5'-GAGGTCTGCGTGAATCCCTA-3',
SPP1 R: 5'-GGAATGGCTGTAGTCGTCCA-3';
α-SMA F: 5'-ACTGCCTTGGTGTGTGACAA-3',
α-SMA R: 5'-CACCATCACCCCCTGATGTC-3';
Collagen I F: 5'-GGGCGAGTGCTGTGCTTT-3',
Collagen I R: 5'-GACCCATTGGACCTGAACC-3'.

Western blot analysis

Cell proteins were extracted with NP-40 Lysis Buffer (Beyotime), and bicinchoninic acid (BCA) assay (Beyotime) was used to determine protein concentration. Sodium dodecyl sulphate-polyacrylamide gel electrophoresis (SDS-PAGE) with 5% stacking gel and 10% separation gel was used to isolate proteins that were transferred to polyvinylidene fluoride (PVDF) membranes. Blots were blocked with 5% skimmed milk for 2 h and incubated with the corresponding primary antibody overnight at 4°C. On the following day, blots were treated with a secondary antibody at room temperature for 2 h and then developed using enhanced chemiluminescence (ECL) reagent (Applygen, Beijing, China). The protein expressions of Collagen I, α-SMA and SPP1 were normalized to GAPDH, while phosphorylated (p)-Smad2/3 were normalized to Smad2/3. Protein expression in the control group was set to 1. The antibodies used to probe the PVDF membranes were as follows: GAPDH (ab9485, 1:5000; Abcam), SPP1 (ab255435, 1:3000; Abcam), Collagen I (ab64883, 1:1500; Abcam), α-SMA (ab244177, 1:1000; Abcam), p-Smad2 (ab188334, 1:3000; Abcam), p-Smad3 (ab48054, 1:3000; Abcam), Smad2 (SRP 12209, 1:2000; Tianjin Saier Biotechnology Co., Ltd., Tianjin, China), and Smad3 (SRP 06283, 1:2000; Tianjin Saier Biotechnology Co., Ltd.).

Cell transfection

The following vectors were used in the present study: pcDNA3/miR-340-5p was used to overexpress miR-340-5p; pcDNA3/SPP1 was used to overexpress SPP1; shR-SPP1 was used to interfere with SPP1 expression; pcDNA3 was used as the negative control (NC) for pcDNA3/miR-340-5p and pcDNA3/SPP1; and pSilencer was used as NC for shR-SPP1. All the vectors were obtained from Tianjin Saier Biotechnology. The LX-2 cells, growing in a 96-well cell culture plates, were transfected with 0.25 μg DNA/well. The miR-340-5p inhibitor and control random sequence inhibitor (NC-inhibitor) (Zhongshi Gene Technology, Tianjin, China) were transfected into LX-2 cells at a final

concentration of 100 nM. All transfections were performed according to the Lipofectamine® 2000 protocol (Thermo Fisher Scientific).

Fluorescent reporter assay

Vector pcDNA3/EGFP-SPP1 3'UTR containing wild-type 3'-untranslated region (UTR) of SPP1 mRNA complementary to miR-340-5p sequence, and pcDNA3/EGFP-SPP1 3'UTR-MUT vector containing mutated 3'UTR of SPP1 mRNA complementary to miR-340-5p sequence, as well as pDsRed2-N1 vector (used as internal control of transfection), were purchased from Clontech Laboratories (Mountain View, USA). The LX-2 cells, growing in a 6-well cell culture plates, were transfected with: 1 µg pcDNA3 or pcDNA3/miR-340-5p, 1 µg pcDNA3/EGFP-SPP1 3'UTR or pcDNA3/EGFP-SPP1 3'UTR-MUT, and 0.1 µg pDsRed2-N1. After 48 h, the cells were treated with lysis buffer (Beyotime), and the fluorescence intensities of enhanced green fluorescent protein (EGFP) and red fluorescent protein (RFP) were determined using an F-4500 fluorescence spectrophotometer (Molecular Devices, San Jose, USA). The fluorescence intensity ratio of EGFP to RFP was calculated to determine the relative fluorescence intensity of the former. The pcDNA3 and pcDNA3/EGFP-SPP1 3'UTR transfection groups were the control for pcDNA3/miR-340-5 and pcDNA3/EGFP-SPP1 3'UTR, while the pcDNA3 and pcDNA3/EGFP-SPP1 3'UTR-MUT transfection groups were the control for pcDNA3/miR-340-5p and pcDNA3/EGFP-SPP1 3'UTR-MUT. The relative fluorescence intensity of EGFP was set to 1 in the control group.

Cell proliferation assay

The cell counting kit-8 (CCK-8) assay (Invitrogen, Thermo Fisher Scientific) was used to determine the proliferation of LX-2 cells. The cells were placed in 96-well plates with DMEM and a total of 3×10^3 cells per well. The pcDNA3/miR-340-5p, pcDNA3, miR-340 inhibitor, or NC-inhibitor were transfected individually with Opti-MEM (Tianjin Meiji Chemical Co., Ltd.), and Lipofectamine® 2000. A total of 100 µL of medium and 10 µL of CCK-8 reagent were added 24 h, 48 h or 72 h after transfection, and the absorbance at 450 nm was determined in each well after a 3-hour incubation.

Statistical analyses

The SPSS v. 26.0 software (IBM Corp., Armonk, USA) was used to analyze the experimental data and GraphPad Prism software (v. 8.0; GraphPad Software, San Diego, USA) was used to present the results. The unpaired Student's t-test bootstrap was used for comparisons between the 2 groups and the one-way analysis of variance (ANOVA) bootstrap followed by the least significant difference (LSD) test or Dunnett T3 post hoc test was used for multiple comparisons among the 4 groups. The Welch's correction was used when the homogeneity of variance assumption was not met, and the data description of statistical test results are shown in Supplementary Tables 1–6 (https://doi.org/10.5281/zenodo.7115492). Seven rats were used for the induced BDL rat model. The other experiments were performed in triplicate. Representative results are shown as mean ± standard deviation (M ±SD), with $p < 0.05$ considered statistically significant.

Results

BDL-induced HF rat model and differential gene expression

Using the BDL rat model, the characteristics of HF were determined. The results showed that the daily growth rate of the BDL group was significantly lower than controls, and the liver wet weight, body mass ratio, ALT, AST, TBA, and TBIL were significantly increased (Table 1). Significant histological changes and deposition of Collagen I were detected in liver tissue sections of BDL rats using H&E, Sirius Red and Masson's trichrome staining when compared to controls (Fig. 1A). In addition, the upregulation of α-SMA in the central venous and portal regions of BDL rat liver tissue sections was observed with immunohistochemical analysis (Fig. 1B).

To systematically identify genes involved in the pathophysiology of HF, the differential gene expression was analyzed in liver tissues of BDL and control rats using mRNA microarray. Two major clusters were identified using unsupervised hierarchical clustering analysis among the differentially expressed mRNAs, with one set closely

Table 1. Liver to body mass ratio and serum biochemical test results of rats in each group

Groups	Growth rate (daily %)	Liver/body weight [g/kg]	Serum ALT [U/L]	Serum AST [U/L]	Serum TBA [µmol/L]	Serum TBIL [U/L]
Sham group (n = 7)	0.39 ±0.05	25.53 ±1.37	45.13 ±1.7	134.03 ±9.53	5.39 ±3.54	10.65 ±1.22
BDL group (n = 7)	0.30 ±0.07	61.99 ±2.49	101.76 ±3.87	438.49 ±14.33	215.17 ±11.39	150.16 ±9.99
Lower limit of the 95% CI	0.0205	–38.3728	–59.5055	–317.2698	–218.8642	–146.4505
Upper limit of the 95% CI	0.1496	–34.2832	–53.2831	–292.6431	–201.0801	–131.8945

The t-test bootstrap was used to compare the difference between the sham group and the bile duct ligation (BDL) group. Each value represents the mean ± standard deviation (M ±SD) of 7 rats. ALT – alanine aminotransferase; AST – aspartate aminotransferase; TBA – total bile acid; TBIL – total bilirubin; 95% CI – 95% confidence interval.

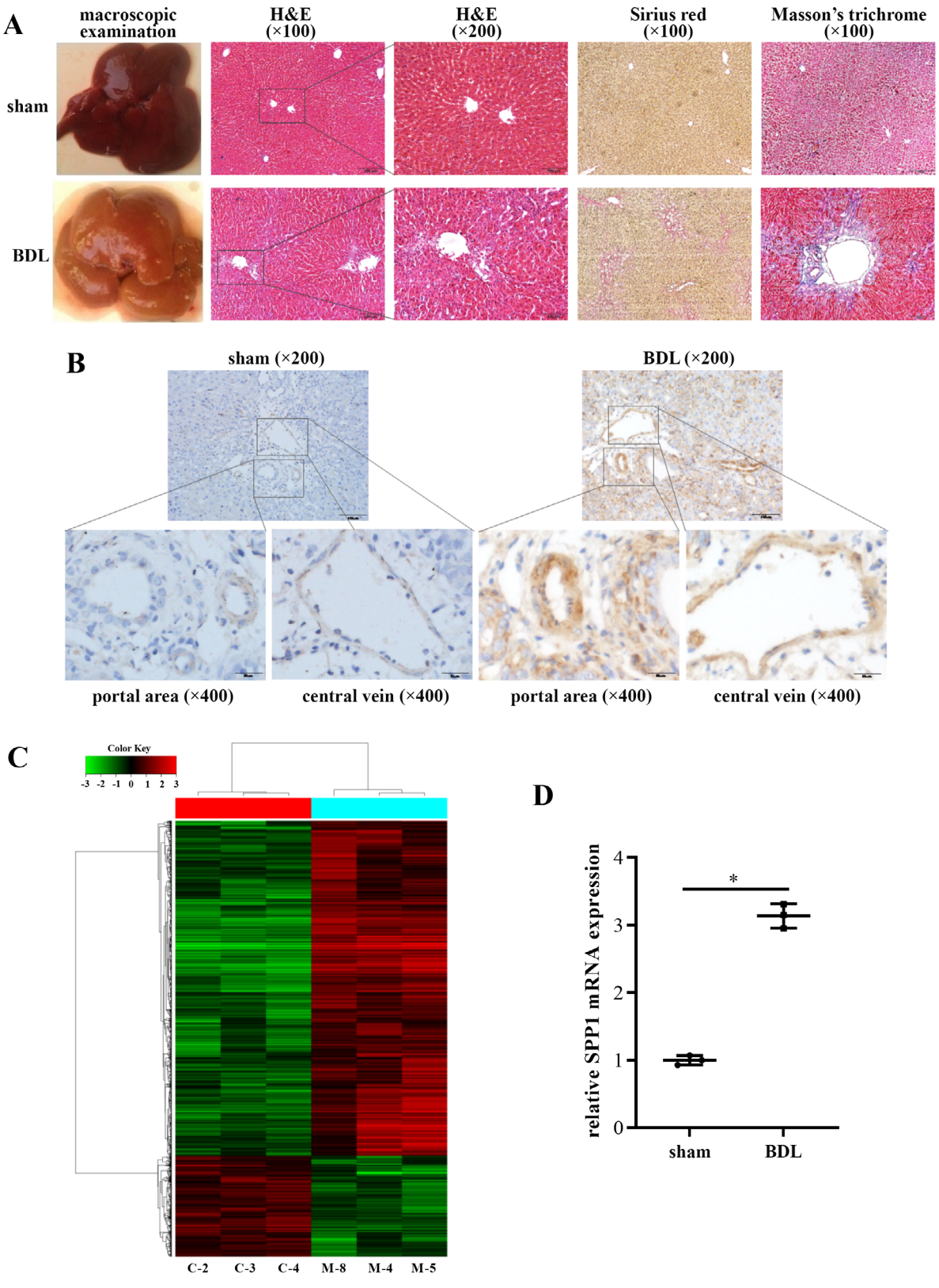

Fig. 1. Differential expression of genes in bile duct ligation (BDL) rat liver. A. Macroscopic examination of rat liver and representative images of hematoxylin and eosin (H&E) staining (×100 and ×200 magnification), Sirius Red staining (×100 magnification), Masson's trichrome staining (×100 magnification) of rat liver tissue sections, n = 7; B. Immunohistochemical staining for alpha smooth muscle actin (α-SMA) in the central vein and portal region of rat liver tissue sections (×200 and ×400 magnification), n = 7; C. Microarray analysis of liver tissue mRNAs in sham or BDL group. Hierarchical cluster analysis was performed for differential expression mRNAs; green – low expression; black – no difference; red – high expression; C-2, C-3 and C-4 are the sham group results; M-4, M-5 and M-8 are the BDL group results, n = 3; D. The expression of secreted phosphoprotein 1 (SPP1) in liver tissues was analyzed with quantitative real-time polymerase chain reaction (qRT-PCR) using samples from the sham and BDL groups. Data for SPP1 were normalized to mRNA expression of glyceraldehyde 3-phosphate dehydrogenase (GAPDH), and the data for the sham group were standardized to 1. Results are shown as mean ± standard deviation (M ±SD), n = 3, *$p < 0.05$ compared to the control; the results were analyzed using the Student's t-test bootstrap

associated with the BDL group and the other with the sham group. Compared to the sham group, there were 1985 upregulated and 598 downregulated mRNAs in the BDL group (Fig. 1C), with SPP1 being one of the most upregulated mRNAs ($p < 0.05$, $n = 3$) (Fig. 1D). The SPP1 is related to the TGF-β1/Smads signaling pathway, as indicated by Kyoto Encyclopedia of Genes and Genomes (KEGG) and Gene Ontology (GO) analyses, which suggests that SPP1 is likely critical in HF.

SPP1 enhances the proliferation and activation of LX-2 cells through promotion of the TGF-β1/Smads signaling pathway

To determine the function and possible mechanism of SPP1 in HF, LX-2 cells and TGF-β1-activated LX-2 cells were used. It is reported that LX-2 cells can be further activated by TGF-β1.[18] The TGF-β1 interacts with receptor II (TGFBR2) on the cell surface, which leads to the phosphorylation of receptor I (TGFBR1). Smad2 and Smad3 are phosphorylated to become p-Smad2 and p-Smad3 by p-TGFBR1, where they form a cytoplasmic heteromeric complex that traffics to the nucleus to mediate HF.[20] This leads to the expression of SPP1 that were detected in activated LX-2 cells. The levels of SPP1 mRNA and protein were significantly enhanced in LX-2 cells treated with TGF-β1, as examined using qRT-PCR and western blot, respectively (all $p < 0.05$, Fig. 2A,B). Additional studies were performed in LX-2 cells by transfecting them with pcDNA3/SPP1, shR-SPP1 or NCs. The levels of SPP1 mRNA and protein in LX-2 cells transfected with pcDNA3/SPP1 or shR-SPP1 were increased or decreased relative to NCs, as detected using qRT-PCR or western blot, respectively (all $p < 0.05$, Fig. 2C,F). The proliferation of LX-2 cells transfected with pcDNA3/SPP1 or shR-SPP1 was significantly increased and decreased relative to controls, respectively, as determined with CCK-8 analysis (all $p < 0.05$, Fig. 2D). Additionally, the mRNA and protein levels of HF markers Collagen I and α-SMA in LX-2 cells transfected with pcDNA3/SPP1 or shR-SPP1 were significantly higher and lower than in their NCs, respectively (all $p < 0.05$, Fig. 2E,F). The protein expression of p-Smad2 and p-Smad3 in LX-2 cells transfected with pcDNA3/SPP1 were increased, while those transfected with shR-SPP1 were decreased when normalized to the total Smad2 or Smad3 protein (all $p < 0.05$, Fig. 2G). Thus, SPP1 might promote HSC proliferation and activation through the TGF-β1/Smads signaling pathway.

SPP1 is directly targeted by miR-340-5p

A growing number of studies have indicated that miRNAs directly interfere with the expression of their target genes, which likely happens in the occurrence and development of HF. Thus, the question of whether SPP1 is regulated by miRNAs was investigated. The results obtained using TargetScan and miRDB database analysis suggested that SPP1 can be directly targeted and regulated by miR-340-5p (Fig. 3A). The cells co-transfected with miR-340-5p and pcDNA3/EGFP-SPP1 3'UTR vector had a decreased fluorescence intensity ($p < 0.05$, Fig. 3B). However, no significant difference was seen in the co-transfection of miR-340-5p and the mutant pcDNA3/EGFP-SPP1 3'UTR-MUT ($p > 0.05$, Fig. 3B). Furthermore, SPP1 mRNA and protein levels in LX-2 cells transfected with pcDNA3/miR-340-5p were significantly decreased, while those with miR-340-5p inhibitor were increased (all $p < 0.05$, Fig. 3C,D). These results suggest that miR-340-5p directly suppresses SPP1 by interfering with its 3'UTR.

miR-340-5p inhibits the proliferation and activation of LX-2 cells by repressing the TGF-β1/Smads pathway

Next, LX-2 cells were used to systematically identify the effects of miR-340-5p in the pathophysiology of HF. The cells were transfected with pcDNA3/miR-340-5p, pcDNA3, miR-340-5p inhibitor or NC-inhibitor, and analyzed for cell proliferation, mRNA and protein expression levels of fibrosis markers Collagen I and α-SMA, as well as protein levels of p-Smad2 and p-Smad3. Compared with TGF-β1-untreated groups, the activated NFs and LX-2 cells had significantly reduced levels of miR-340-5p ($p < 0.05$, Fig. 4A). Also, the expression of miR-340-5p in LX-2 was dramatically enhanced and decreased by the transfection of its overexpression vectors and inhibitors, respectively (both $p < 0.05$, Fig. 4B). The proliferation of LX-2 cells was strikingly inhibited and promoted by pcDNA3/miR-340-5p and miR-340-5p inhibitor, respectively (all $p < 0.05$, Fig. 4C). Collagen I, α-SMA mRNA and protein levels were significantly downregulated by pcDNA3/miR-340-5p and significantly upregulated by miR-340-5p inhibitor (all $p < 0.05$, Fig. 4D,E). Additionally, the levels of p-Smad2 and p-Smad3 were reduced with pcDNA3/miR-340-5p or increased with miR-340-5p inhibitor (all $p < 0.05$, Fig. 4F), when normalized to total protein Smad2 or Smad3. These findings suggest that miR-340-5p inhibits the proliferation and activation of LX-2 cells by inhibiting the TGF-β1/Smads canonical pathway (Fig. 5).

Discussion

Factors such as viral infection, alcohol abuse and metabolic or genetic disorders cause HF, and its main characteristic is ECM protein accumulation, including Collagen I and α-SMA. Activated HSCs are responsible for the excessive ECM protein accumulation.[21] Hepatic stellate cells, which account for approx. 5% of all hepatocytes, were first described by Kupffer in 1876, and they exist in the space between parenchymal cells, hepatocytes and sinusoidal endothelial cells.[22] They participate in liver development,

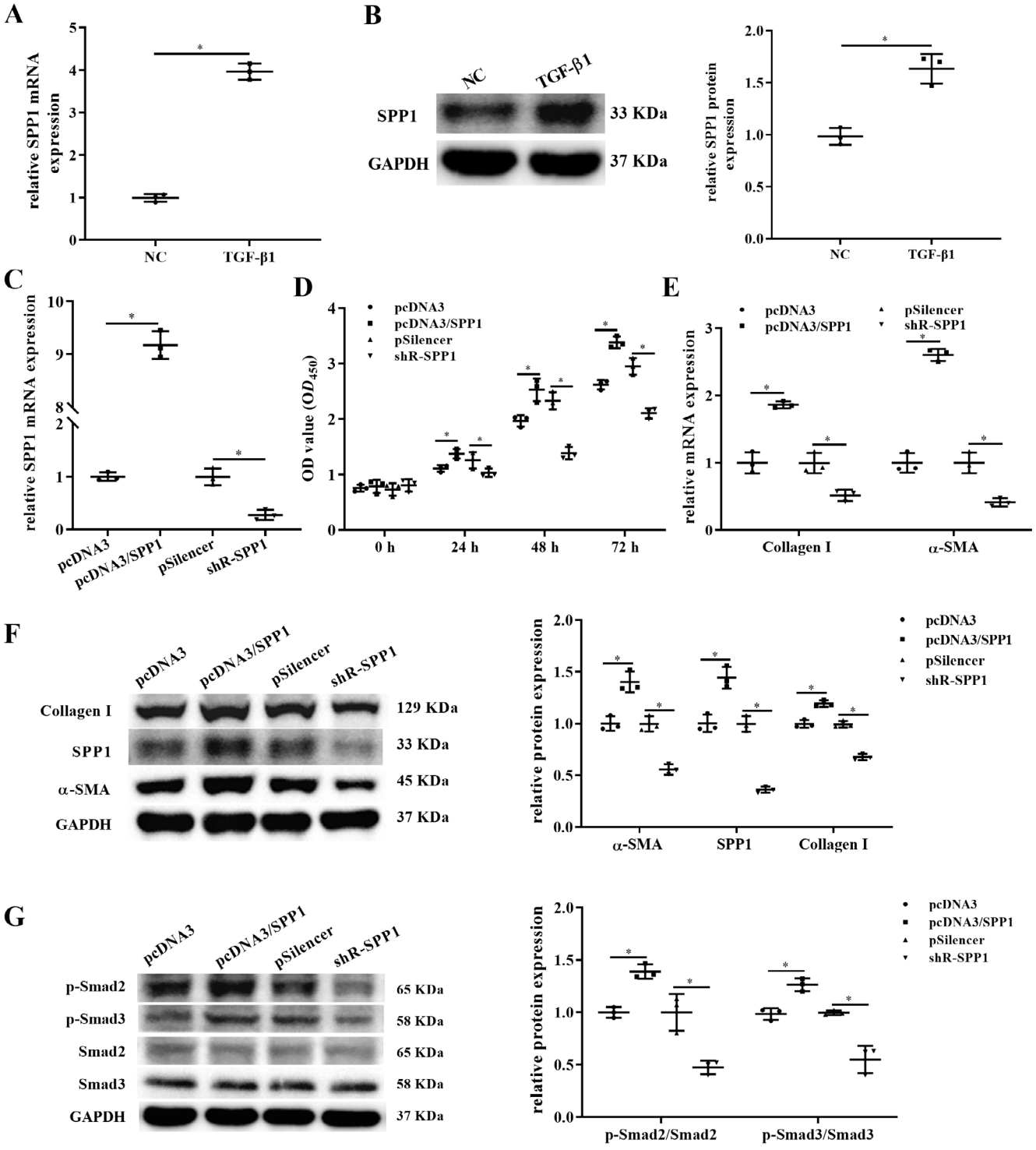

Fig. 2. Secreted phosphoprotein 1 (SPP1) promotes hepatic stellate cell (HSC) proliferation and activation. A. The SPP1 mRNA expression in activated LX-2 cells was examined using quantitative real-time polymerase chain reaction (qRT-PCR); B. The SPP1 protein expression in transforming growth factor beta 1 (TGF-β1)-activated LX-2 cells was examined with western blot; C. The SPP1 mRNA expression in LX-2 cells transfected with pcDNA3/SPP1 or shR-SPP1 was quantified using qRT-PCR; D. The proliferation of LX-2 cells transfected with pcDNA3/SPP1 or shR-SPP1 was determined using cell counting kit-8 (CCK-8) assay; E. The mRNA expression levels of Collagen I and alpha smooth muscle actin (α-SMA) in LX-2 cells transfected with pcDNA3/SPP1 or shR-SPP1 were quantified using qRT-PCR; F. The protein expression levels of Collagen I, α-SMA and SPP1 in LX-2 cells transfected with pcDNA3/SPP1 or shR-SPP1 were determined with western blot; G. Phosphorylated (p)-Smad2 and p-Smad3 expression levels were determined using western blot in LX-2 cells transfected with pcDNA3/SPP1 or shR-SPP1, which were normalized to the total Smad2 or Smad3, respectively. The gene expression levels in LX-2 cells transfected with pcDNA3 or pSilencer were normalized to 1; glyceraldehyde 3-phosphate dehydrogenase (GAPDH) was used for internal control. Results are shown as mean ± standard deviation (M ±SD), n = 3, *p < 0.05 compared to the control; the results were analyzed using the Student's t-test bootstrap or one-way analysis of variance (ANOVA) bootstrap followed by least significant difference (LSD) test or Dunnett T3 post hoc test

NC – negative control; TGF-β1 – transforming growth factor beta 1; OD – optical density.

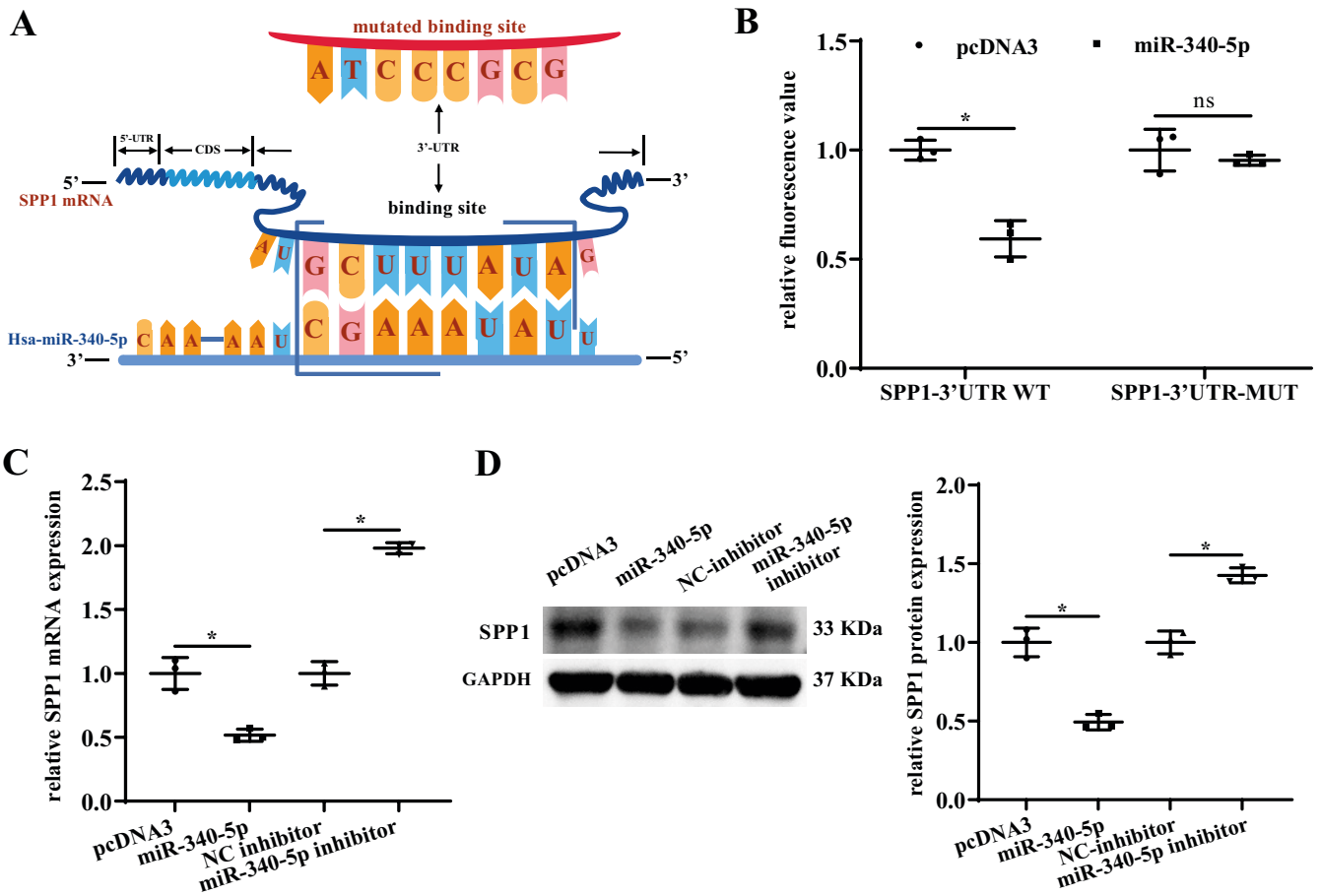

Fig. 3. Secreted phosphoprotein 1 (SPP1) is the target of miR-340-5p. A. miR-340-5p binding site and the mutated binding site in SPP1 3'UTR; B. LX-2 cells were transfected with pcDNA3/miR-340-5p and SPP1-3'UTR WT or MUT, and the enhanced green fluorescence protein (EGFP) intensity was determined and normalized to 1 in the control group; C,D. mRNA and protein expression levels of SPP1 in LX-2 cells transfected with pcDNA3/miR-340-5p or miR-340-5p inhibitor were detected using quantitative real-time polymerase chain reaction (qRT-PCR) and western blot. The mRNA levels in LX-2 cells transfected with pcDNA3 or NC-inhibitor were normalized to 1, glyceraldehyde 3-phosphate dehydrogenase (GAPDH) was used for internal control. Results are shown as mean ± standard deviation (M ±SD), n = 3, ns – not significant, *p < 0.05 compared to the control. The results were analyzed using one-way analysis of variance (ANOVA) bootstrap followed by least significant difference (LSD) post hoc test

differentiation, regeneration, immune regulation, inflammatory response, and liver blood flow control, as well as regulate the occurrence and development of some liver diseases. Once a liver injury occurs, quiescent HSCs are activated and transformed into contractile myofibroblasts, which induce the transcription of Collagen I and α-SMA, and lead to the formation of stress fibers and ECM deposition, which results in increased cell contact.[23] Since the complexity of HSC activation and the pathogenesis of HF are not fully understood, it is critical to clarify the regulatory mechanisms, so as to improve the treatment options for HF.

The *SPP1* gene is on chromosome 4 (4q13) and encodes a multifunctional matricellular protein that is abundantly expressed during inflammation and repair.[24] The *SPP1* also promotes inflammation and fibrosis of the prostate,[25] as well as aggravates the lungs[26] and promotes myocardial fibrosis[27] through different signaling pathways. It is known to regulate radiotherapy sensitivity in gastric adenocarcinoma through the Wnt/β-catenin pathway.[28] Similarly, our results revealed that a high expression of *SPP1* occurs in fibrotic liver tissue of BDL rats and activated LX-2 cells, and it is related to the TGF-β1/Smads signaling pathway, as indicated by KEGG and GO analysis.

Hepatic stellate cells gradually become activated during culturing in vitro, and LX-2 cells used in these experiments are an activated immortalized cell line.[29,30] Therefore, LX-2 cells were used to study SPP1 in order to avoid the influence of exogenous TGF-β1. These studies showed an increase in the levels of mRNA and protein for the markers of HF (Collagen I and α-SMA), as well as the proteins p-Smad2 and p-Smad3, with proliferation occurring when LX-2 cells overexpressed SPP1.

The results of the bioinformatics prediction combined with fluorescence reporter studies showed that SPP1 is the target of miR-340-5p. This is the first study to report on the effect of miR-340-5p in HF. Additional experiments showed that the expression of miR-340-5p was significantly downregulated both in the activated NFs and the activated LX-2 cells. Also, when pcDNA3/

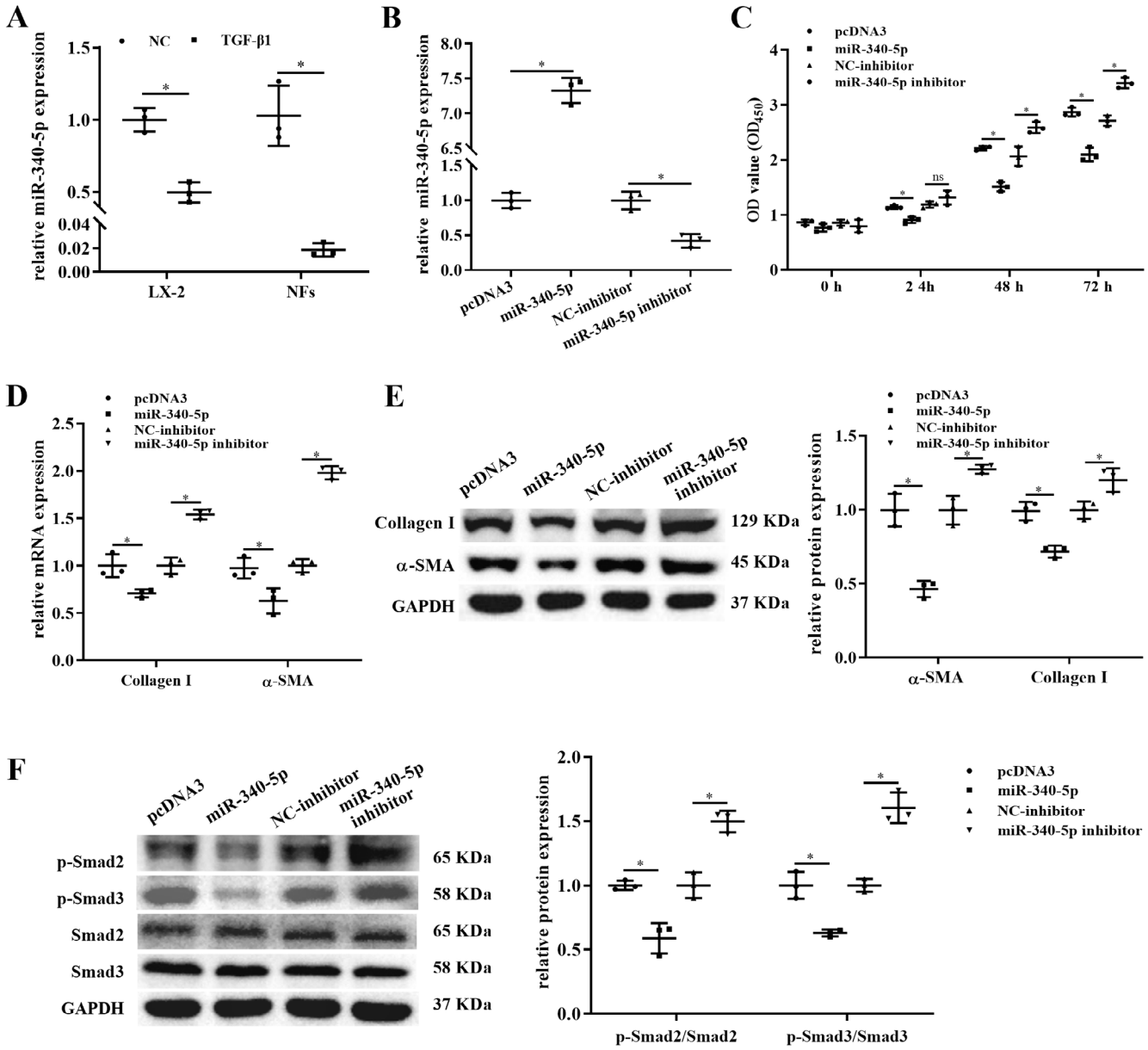

Fig. 4. The miR-340-5p inhibits hepatic stellate cell (HSC) proliferation and activation. A. Expression of miR-340-5p in activated normal fibroblasts (NFs) and activated LX-2 cells was detected using quantitative real-time polymerase chain reaction (qRT-PCR); B. The expression of miR-340-5p in LX-2 cells transfected with pcDNA3/miR-340-5p or miR-340-5p inhibitor was quantified using qRT-PCR; C. Cell proliferation was determined using cell counting kit-8 (CCK-8) assay in LX-2 cells transfected with either pcDNA3/miR-340-5p or miR-340-5p inhibitor; D,E. The mRNA and protein expression levels of Collagen I and alpha smooth muscle actin (α-SMA) in LX-2 cells transfected with pcDNA3/miR-340-5p or miR-340-5p inhibitor were detected using qRT-PCR and western blot; F. The levels of p-Smad2 and p-Smad3 were detected using western blot in LX-2 cells transfected with pcDNA3/miR-340-5p or miR-340-5p inhibitor, which were normalized to the total Smad2 or Smad3 protein. The gene expression in LX-2 cells transfected with pcDNA3 or NC-inhibitor were normalized to 1; U6 was used as the internal reference for miR-340-5p and glyceraldehyde 3-phosphate dehydrogenase (GAPDH) was used as the internal reference for Collagen I, α-SMA, p-Smad2, and p-Smad3. Results are shown as mean ± standard deviation (M ±SD), n = 3, ns – not significant, *p < 0.05 compared to the control. The results were analyzed using one-way analysis of variance (ANOVA) bootstrap followed by least significant difference (LSD) or Dunnett T3 post hoc test

NC – negative control; OD – optical density; TGF-β1 – transforming growth factor beta 1.

miR-340-5p or miR-340-5p inhibitor was transfected into LX-2 cells to upregulate or knock down the expression of miR-340-5p, respectively, the proliferation of LX-2 cells was significantly downregulated with high levels of miR-340-5p, and upregulated with low levels of miR-340-5p in LX-2 cells. These results, along with the changes to HF markers Collagen I, α-SMA, p-Smad2, and p-Smad3, suggest altered levels of SPP1.

Limitations

In this study, we only carried out cellular experiments to investigate the effect of miR-340-5p on LX-2 cell proliferation and activation by targeting SPP1, there should be some focus on validating these findings in vivo. Therefore, animal experiments and clinical HF tissue samples are needed to confirm the effect of miR-340-5p on HF.

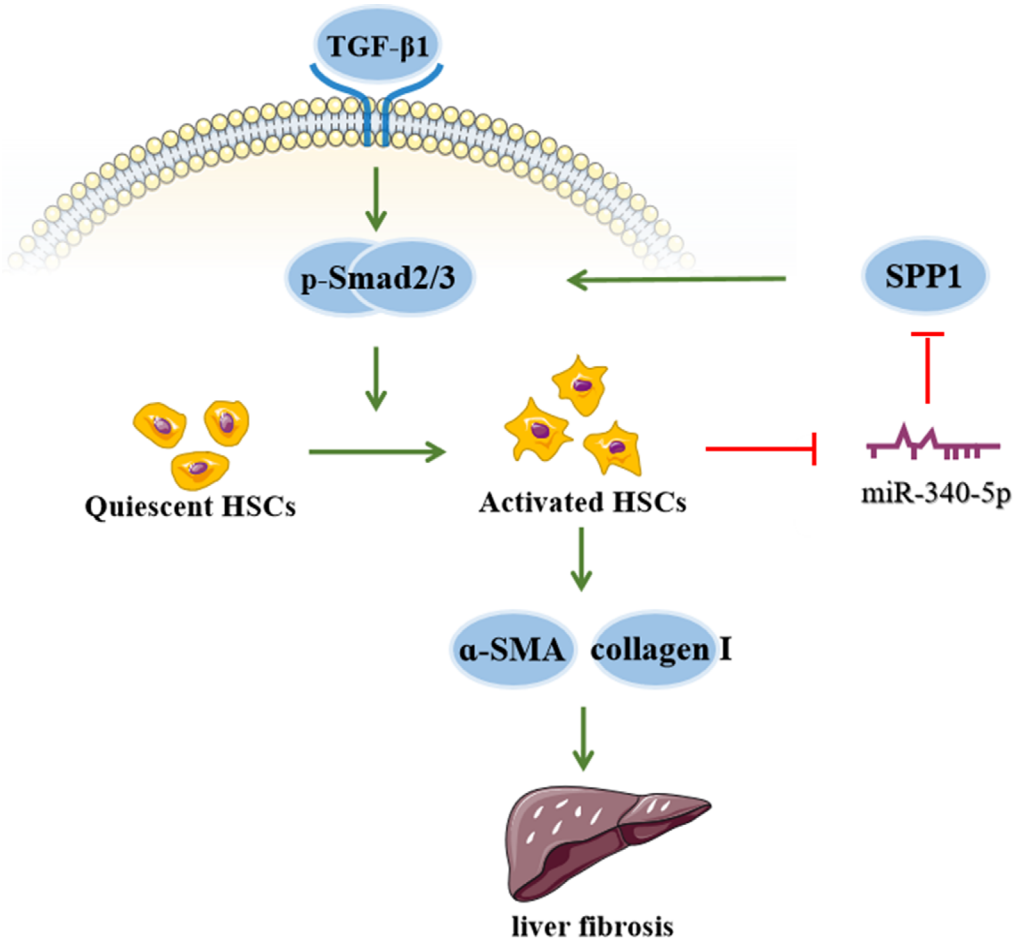

Fig. 5. Schematic representation of a working model of how miR-340-5p suppresses hepatic stellate cell (HSC) activation via the inhibition of the transforming growth factor beta 1 (TGF-β1)/Smads signaling pathway

SPP1 – secreted phosphoprotein 1; α-SMA – alpha smooth muscle actin.

Conclusions

Our findings provide evidence that SPP1 promotes LX-2 cell proliferation and activation through TGF-β1/Smads signaling and that it is the target of miR-340-5p. Therefore, miR-340-5p and SPP1 may be potential therapeutic targets for HF. However, in vivo studies are needed to evaluate the effect of miR-340-5p and SPP1 on HF.

Supplementary materials

The supplementary materials are available at https://doi.org/10.5281/zenodo.7115492.

Supplementary Table 1. Results of t-test bootstrap presented in Table 1.

Supplementary Table 2. Results of t-test bootstrap presented in Fig. 1D.

Supplementary Table 3. Results of t-test bootstrap presented in Fig. 2A,B.

Supplementary Table 4. Results of one-way ANOVA bootstrap followed by post hoc test presented in Fig. 2C–G

Supplementary Table 5. Results of one-way ANOVA bootstrap followed by post hoc test presented in Fig. 3B–D

Supplementary Table 6. Results of one-way ANOVA bootstrap followed by post hoc test presented in Fig. 4A–F.

ORCID iDs

Ronghua Zhang https://orcid.org/0000-0003-2433-1288
Meimei Wang https://orcid.org/0000-0001-9357-8466
Hongjian Lu https://orcid.org/0000-0002-0345-6500
Jingyao Wang https://orcid.org/0000-0003-3684-120X
Xiangyang Han https://orcid.org/0000-0001-7189-5700
Zhiyong Liu https://orcid.org/0000-0003-0900-2275
Lin Li https://orcid.org/0000-0002-1759-7582
Mingming Li https://orcid.org/0000-0001-9922-0940
Xiaoli Tian https://orcid.org/0000-0002-1609-131X
Shuang Chen https://orcid.org/0000-0001-5254-6353
Guangling Zhang https://orcid.org/0000-0002-9542-4986
Yanan Xiong https://orcid.org/0000-0002-5638-4889
Jingwu Li https://orcid.org/0000-0002-7851-5624

References

1. Zhou L, Liu S, Han M, et al. miR-185 inhibits fibrogenic activation of hepatic stellate cells and prevents liver fibrosis. *Mol Ther Nucleic Acids*. 2018;10:91–102. doi:10.1016/j.omtn.2017.11.010
2. Xu Y, Sun X, Zhang R, et al. A positive feedback loop of TET3 and TGF-β1 promotes liver fibrosis. *Cell Rep*. 2020;30(5):1310.e5–1318.e5. doi:10.1016/j.celrep.2019.12.092
3. Hata A, Chen YG. TGF-β signaling from receptors to Smads. *Cold Spring Harb Perspect Biol*. 2016;8(9):a022061. doi:10.1101/cshperspect.a022061
4. Aydin MM, Akcali KC. Liver fibrosis. *Turk J Gastroenterol*. 2018;29(1):14–21. doi:10.5152/tjg.2018.17330
5. Xu X, Hong P, Wang Z, Tang Z, Li K. MicroRNAs in transforming growth factor-beta signaling pathway associated with fibrosis involving different systems of the human body. *Front Mol Biosci*. 2021;8:707461. doi:10.3389/fmolb.2021.707461
6. Tao L, Xue D, Shen D, et al. MicroRNA-942 mediates hepatic stellate cell activation by regulating BAMBI expression in human liver fibrosis. *Arch Toxicol*. 2018;92(9):2935–2946. doi:10.1007/s00204-018-2278-9

7. Wei S, Wang Q, Zhou H, et al. miR-455-3p alleviates hepatic stellate cell activation and liver fibrosis by suppressing HSF1 expression. *Mol Ther Nucleic Acids*. 2019;16:758–769. doi:10.1016/j.omtn.2019.05.001
8. Wei YQ, Guo YF, Yang SM, Ma HH, Li J. MiR-340-5p mitigates the proliferation and activation of fibroblast in lung fibrosis by targeting TGF-β/p38/ATF1 signaling pathway. *Eur Rev Med Pharmacol Sci*. 2020; 24(11):6252–6261. doi:10.26355/eurrev_202006_21523
9. Xiao B, Zhu Y, Huang J, Wang T, Wang F, Sun S. Exosomal transfer of bone marrow mesenchymal stem cells-derived miR340 attenuates endometrial fibrosis. *Biol Open*. 2019;8(5):bio.039958. doi:10.1242/bio.039958
10. On behalf of the AGIMM (AIRC Gruppo Italiano Malattie Mieloproliferative) Investigators; Ruberti S, Bianchi E, Gugliemelli P, et al. Involvement of MAF/SPP1 axis in the development of bone marrow fibrosis in PMF patients. *Leukemia*. 2018;32(2):438–449. doi:10.1038/leu.2017.220
11. Morse C, Tabib T, Sembrat J, et al. Proliferating SPP1/MERTK-expressing macrophages in idiopathic pulmonary fibrosis. *Eur Respir J*. 2019; 54(2):1802441. doi:10.1183/13993003.02441-2018
12. Dong J, Ma Q. Osteopontin enhances multi-walled carbon nanotube-triggered lung fibrosis by promoting TGF-β1 activation and myofibroblast differentiation. *Part Fibre Toxicol*. 2017;14(1):18. doi:10.1186/s12989-017-0198-0
13. Zhang Y, Tang Y, Yan JH. LncRNA-XIST promotes proliferation and migration in ox-LDL stimulated vascular smooth muscle cells through miR-539-5p/SPP1 axis. *Oxid Med Cell Longev*. 2022;2022:9911982. doi:10.1155/2022/9911982
14. Lin Z, Tian X, Huang X, He L, Xu F. microRNA-186 inhibition of PI3K–AKT pathway via SPP1 inhibits chondrocyte apoptosis in mice with osteoarthritis. *J Cell Physiol*. 2019;234(5):6042–6053. doi:10.1002/jcp.27225
15. Wang J, Hao F, Fei X, Chen Y. SPP1 functions as an enhancer of cell growth in hepatocellular carcinoma targeted by miR-181c. *Am J Transl Res*. 2019;11(11):6924–6937. PMID:31814897.
16. Huang H, Wang XP, Li XH, et al. Prognostic value of pretreatment serum alanine aminotransferase/aspartate aminotransferase (ALT/AST) ratio and gamma glutamyltransferase (GGT) in patients with esophageal squamous cell carcinoma. *BMC Cancer*. 2017;17(1):544. doi:10.1186/s12885-017-3523-y
17. Zheng X, Li JW, Liu YK, et al. microRNA-10a-5p overexpression suppresses malignancy of colon cancer by regulating human liver cancer fibroblasts. *Neoplasma*. 2021;68(6):1157–1168. doi:10.4149/neo_2021_210226N250
18. Cho SS, Lee JH, Kim KM, et al. REDD1 attenuates hepatic stellate cell activation and liver fibrosis via inhibiting of TGF-β/Smad signaling pathway. *Free Radic Biol Med*. 2021;176:246–256. doi:10.1016/j.freeradbiomed.2021.10.002
19. Rehmsmeier M, Steffen P, Höchsmann M, Giegerich R. Fast and effective prediction of microRNA/target duplexes. *RNA*. 2004;10(10):1507–1517. doi:10.1261/rna.5248604
20. Tzavlaki K, Moustakas A. TGF-β signaling. *Biomolecules*. 2020;10(3):487. doi:10.3390/biom10030487
21. Herrera J, Henke CA, Bitterman PB. Extracellular matrix as a driver of progressive fibrosis. *J Clin Invest*. 2018;128(1):45–53. doi:10.1172/JCI93557
22. Sufleţel RT, Melincovici CS, Gheban BA, Toader Z, Mihu CM. Hepatic stellate cells – from past till present: Morphology, human markers, human cell lines, behavior in normal and liver pathology. *Rom J Morphol Embryol*. 2021;61(3):615–642. doi:10.47162/RJME.61.3.01
23. Khomich O, Ivanov AV, Bartosch B. Metabolic hallmarks of hepatic stellate cells in liver fibrosis. *Cells*. 2019;9(1):24. doi:10.3390/cells9010024
24. Göthlin Eremo A, Lagergren K, Othman L, Montgomery S, Andersson G, Tina E. Evaluation of SPP1/osteopontin expression as predictor of recurrence in tamoxifen treated breast cancer. *Sci Rep*. 2020;10(1): 1451. doi:10.1038/s41598-020-58323-w
25. Popovics P, Jain A, Skalitzky KO, et al. Osteopontin deficiency ameliorates prostatic fibrosis and inflammation. *Int J Mol Sci*. 2021;22(22): 12461. doi:10.3390/ijms222212461
26. Kumar A, Elko E, Bruno SR, et al. Inhibition of PDIA3 in club cells attenuates osteopontin production and lung fibrosis. *Thorax*. 2022; 77(7):669–678. doi:10.1136/thoraxjnl-2021-216882
27. Wang X, Li H, Zhang A, et al. Diversity among differentially expressed genes in atrial appendages of atrial fibrillation: The role and mechanism of SPP1 in atrial fibrosis. *Int J Biochem Cell Biol*. 2021;141:106074. doi:10.1016/j.biocel.2021.106074
28. Sun G, Shang Z, Liu W. SPP1 regulates radiotherapy sensitivity of gastric adenocarcinoma via the Wnt/beta-catenin pathway. *J Oncol*. 2021;2021:1642852. doi:10.1155/2021/1642852
29. Mejias M, Gallego J, Naranjo-Suarez S, et al. CPEB4 increases expression of PFKFB3 to induce glycolysis and activate mouse and human hepatic stellate cells, promoting liver fibrosis. *Gastroenterology*. 2020; 159(1):273–288. doi:10.1053/j.gastro.2020.03.008
30. Taimr P. Activated stellate cells express the TRAIL receptor-2/death receptor-5 and undergo TRAIL-mediated apoptosis. *Hepatology*. 2003; 37(1):87–95. doi:10.1053/jhep.2003.50002